Fatigue Performance of High-Frequency Welded Steel I-Beams

PUBLICATION NO. FHWA-HRT-17-110 FEBRUARY 2018

U.S. Department of Transportation
Federal Highway Administration

Research, Development, and Technology
Turner-Fairbank Highway Research Center
6300 Georgetown Pike
McLean, VA 22101-2296

FOREWORD

This report documents limited fatigue testing of I-beams where webs and flanges were joined together with a solid-state, high-frequency welding process. The results of the testing show these beams have commensurate fatigue strength with those welded using traditional fusion welding processes. Solid-state welding offers the advantage of faster welding speed with less heat input, resulting in less distortion, which would be of benefit to the steel fabrication industry. The results of this work would benefit those interested in the fatigue behavior of welded beams used in the construction of steel bridges, including State transportation departments, researchers, and design consultants.

Cheryl Allen Richter, Ph.D., P.E.
Director, Office of Infrastructure
Research and Development

TECHNICAL REPORT DOCUMENTATION PAGE

<table>
<tr><td>1. Report No.
FHWA-HRT-17-110</td><td>2. Government Accession No.</td><td colspan="2">3. Recipient's Catalog No.</td></tr>
<tr><td colspan="2" rowspan="2">4. Title and Subtitle
Fatigue Performance of High-Frequency Welded Steel I-Beams</td><td colspan="2">5. Report Date
January 2018</td></tr>
<tr><td colspan="2">6. Performing Organization Code:</td></tr>
<tr><td colspan="2">7. Author(s)
Benjamin Cross, Ph.D., and Justin Ocel, Ph.D., P.E.</td><td colspan="2">8. Performing Organization Report No.</td></tr>
<tr><td colspan="2" rowspan="2">9. Performing Organization Name and Address
Professional Service Industries, Inc.
13873 Park Center Road, Suite 315
Herndon, VA 20171</td><td colspan="2">10. Work Unit No.</td></tr>
<tr><td colspan="2">11. Contract or Grant No.
DTFH61-10-D-00017</td></tr>
<tr><td colspan="2" rowspan="2">12. Sponsoring Agency Name and Address
Office of Infrastructure Research and Development
Federal Highway Administration
6300 Georgetown Pike
McLean, VA 22101-2296</td><td colspan="2">13. Type of Report and Period Covered
Final Report; June 2013–June 2016</td></tr>
<tr><td colspan="2">14. Sponsoring Agency Code
HRDI-40</td></tr>
<tr><td colspan="4">15. Supplementary Notes
The FHWA Contracting Officer's Representative for this report was Fassil Beshah (HRDI-40).</td></tr>
<tr><td colspan="4">16. Abstract
Fatigue is an important consideration in the design of steel bridges. Historically, the fatigue strength of welded details has been based on full-scale experimental testing. This work looked at the fatigue strength of I-beams that used solid-state, high-frequency welds to make the web-to-flange welds, where traditionally this would be performed with fusion welding processes. The specimens closely replicated those used to derive the current category B classification of web-to-flange welds. The limited fatigue testing demonstrated the fatigue resistance was approximately category B; however, it is only based on three specimens, and additional testing is warranted.</td></tr>
<tr><td colspan="2">17. Key Words
Steel bridges, fatigue, solid-state welding, high-frequency welding</td><td colspan="2">18. Distribution Statement
No restrictions. This document is available through the National Technical Information Service, Springfield, VA 22161.
http://www.ntis.gov</td></tr>
<tr><td>19. Security Classif. (of this report)
Unclassified</td><td>20. Security Classif. (of this page)
Unclassified</td><td>21. No. of Pages
25</td><td>22. Price
N/A</td></tr>
</table>

Form DOT F 1700.7 (8-72) Reproduction of completed page authorized.

SI* (MODERN METRIC) CONVERSION FACTORS

APPROXIMATE CONVERSIONS TO SI UNITS

Symbol	When You Know	Multiply By	To Find	Symbol
		LENGTH		
in	inches	25.4	millimeters	mm
ft	feet	0.305	meters	m
yd	yards	0.914	meters	m
mi	miles	1.61	kilometers	km
		AREA		
in^2	square inches	645.2	square millimeters	mm^2
ft^2	square feet	0.093	square meters	m^2
yd^2	square yard	0.836	square meters	m^2
ac	acres	0.405	hectares	ha
mi^2	square miles	2.59	square kilometers	km^2
		VOLUME		
fl oz	fluid ounces	29.57	milliliters	mL
gal	gallons	3.785	liters	L
ft^3	cubic feet	0.028	cubic meters	m^3
yd^3	cubic yards	0.765	cubic meters	m^3
		NOTE: volumes greater than 1000 L shall be shown in m^3		
		MASS		
oz	ounces	28.35	grams	g
lb	pounds	0.454	kilograms	kg
T	short tons (2000 lb)	0.907	megagrams (or "metric ton")	Mg (or "t")
		TEMPERATURE (exact degrees)		
^oF	Fahrenheit	5 (F-32)/9 or (F-32)/1.8	Celsius	^oC
		ILLUMINATION		
fc	foot-candles	10.76	lux	lx
fl	foot-Lamberts	3.426	candela/m^2	cd/m^2
		FORCE and PRESSURE or STRESS		
lbf	poundforce	4.45	newtons	N
lbf/in^2	poundforce per square inch	6.89	kilopascals	kPa

APPROXIMATE CONVERSIONS FROM SI UNITS

Symbol	When You Know	Multiply By	To Find	Symbol
		LENGTH		
mm	millimeters	0.039	inches	in
m	meters	3.28	feet	ft
m	meters	1.09	yards	yd
km	kilometers	0.621	miles	mi
		AREA		
mm^2	square millimeters	0.0016	square inches	in^2
m^2	square meters	10.764	square feet	ft^2
m^2	square meters	1.195	square yards	yd^2
ha	hectares	2.47	acres	ac
km^2	square kilometers	0.386	square miles	mi^2
		VOLUME		
mL	milliliters	0.034	fluid ounces	fl oz
L	liters	0.264	gallons	gal
m^3	cubic meters	35.314	cubic feet	ft^3
m^3	cubic meters	1.307	cubic yards	yd^3
		MASS		
g	grams	0.035	ounces	oz
kg	kilograms	2.202	pounds	lb
Mg (or "t")	megagrams (or "metric ton")	1.103	short tons (2000 lb)	T
		TEMPERATURE (exact degrees)		
^oC	Celsius	1.8C+32	Fahrenheit	^oF
		ILLUMINATION		
lx	lux	0.0929	foot-candles	fc
cd/m^2	candela/m^2	0.2919	foot-Lamberts	fl
		FORCE and PRESSURE or STRESS		
N	newtons	0.225	poundforce	lbf
kPa	kilopascals	0.145	poundforce per square inch	lbf/in^2

*SI is the symbol for the International System of Units. Appropriate rounding should be made to comply with Section 4 of ASTM E380.
(Revised March 2003)

TABLE OF CONTENTS

LIST OF FIGURES

LIST OF TABLES

LIST OF ABBREVIATIONS

AASHTO	American Association of State Highway and Transportation Officials
CJP	complete joint penetration
HF	high-frequency

INTRODUCTION

High-frequency (HF) welding is a solid-state welding process that is also referred to as "electrical resistance welding." HF currents heat up the surfaces to be joined together near their melting point; then, the surfaces are mechanically forced, or forged, together to form a welded joint.

Compared to conventional processes, HF welding is extremely fast and does not require welding consumables. For bridge fabrication, the I-shape is of interest. I-shapes can be hot-rolled or built up from three plates welded together with two joints. Using a conventional weld process, three plates are joined with four fillet or partial-penetration welds, two at each web and flange intersection. To orient the molten weld pool most favorably to gravity, likely only two welds can be made simultaneously; then, the work piece is flipped to finish the remaining two welds. With HF welding and dedicated fixturing, however, three plates are simultaneously brought into alignment and HF welded together through the creation of two complete joint penetration (CJP) welds. The HF CJP welds may lead to less injurious weld defects than fusion welds, and less heat input leads to less distortion of the work piece and smaller heat-affected zones. The speed of HF welding is at least an order of magnitude greater than conventional processes.

The primary objective of the research performed in this study was to evaluate the fatigue performance of HF-welded steel I-beams and make recommendations for the use of such I-beams in bridge design that are consistent with current practice. Stated more specifically, the desire was to make a preliminary determination of which American Association of State Highway and Transportation Officials (AASHTO) fatigue design category is appropriate for use in the design of HF-welded steel I-beams in resisting load-induced fatigue failure.(1) This was accomplished by performing fatigue testing on a series of six beam specimens with identical nominal dimensions and steel specification. All testing was conducted at the Federal Highway Administration Turner–Fairbank Highway Research Center.

SPECIMENS

Six HF-welded, doubly symmetric I-beams consisting of ASTM A769 grade 50 steel were attained to be fatigue tested.(2) The specimens were identified sequentially as beam 1 through beam 6. The nominal geometric properties of the steel I-beams are given in table 1. A picture of a representative partial beam cross section (one flange and most of the web) is shown in figure 1. Most noticeable in this picture is the horizontal offset of the web; while it is joined at the midwidth of the flange, the forging force during welding caused a shift in the web to the left. This distortion of the cross section was observed in all the beams and did cause stability issues that will be described in more depth later. The weld itself, shown in figure 2, appeared very uniform, though the manufacturer of this I-beam did not remove the flash that is ejected from the forging event, and this is noted in the figure and highlighted, as it did affect results described later.

Table 1. Beam specimen nominal geometric properties.

Geometric Property	Nominal Value
Beam length, L	144 inches
Flange thickness, t_f	0.35 inch
Flange width, b_f	7.9 inches
Web thickness, t_w	0.24 inch
Web height, h_w	15.7 inches
Area, A	9.3 inches^2
Moment of inertia, I	432.0 inches^4
Section modulus, S	55.0 inches^3

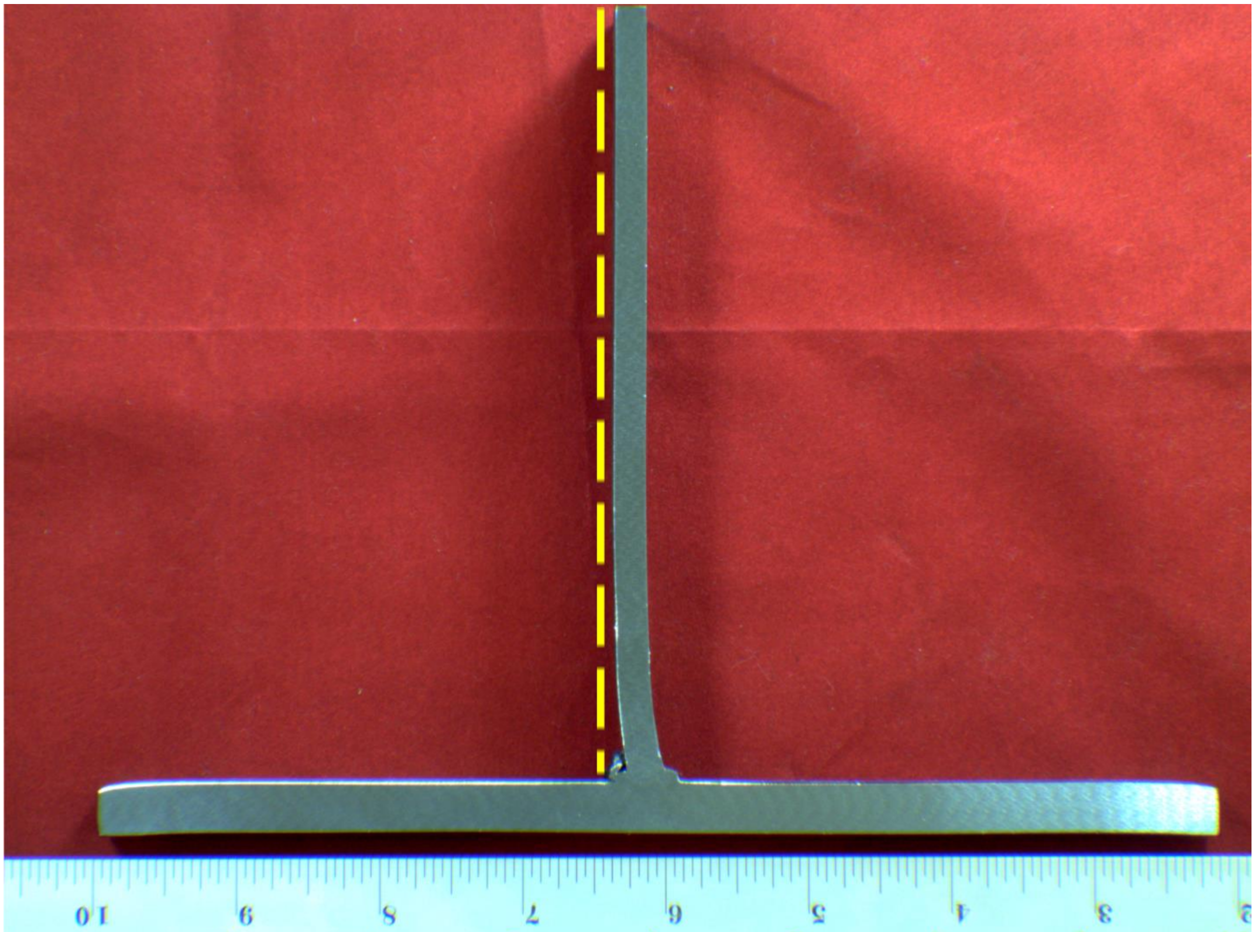

Source: FHWA.
Note: Scale is in units of inches.

Figure 1. Photo. Beam cross section.

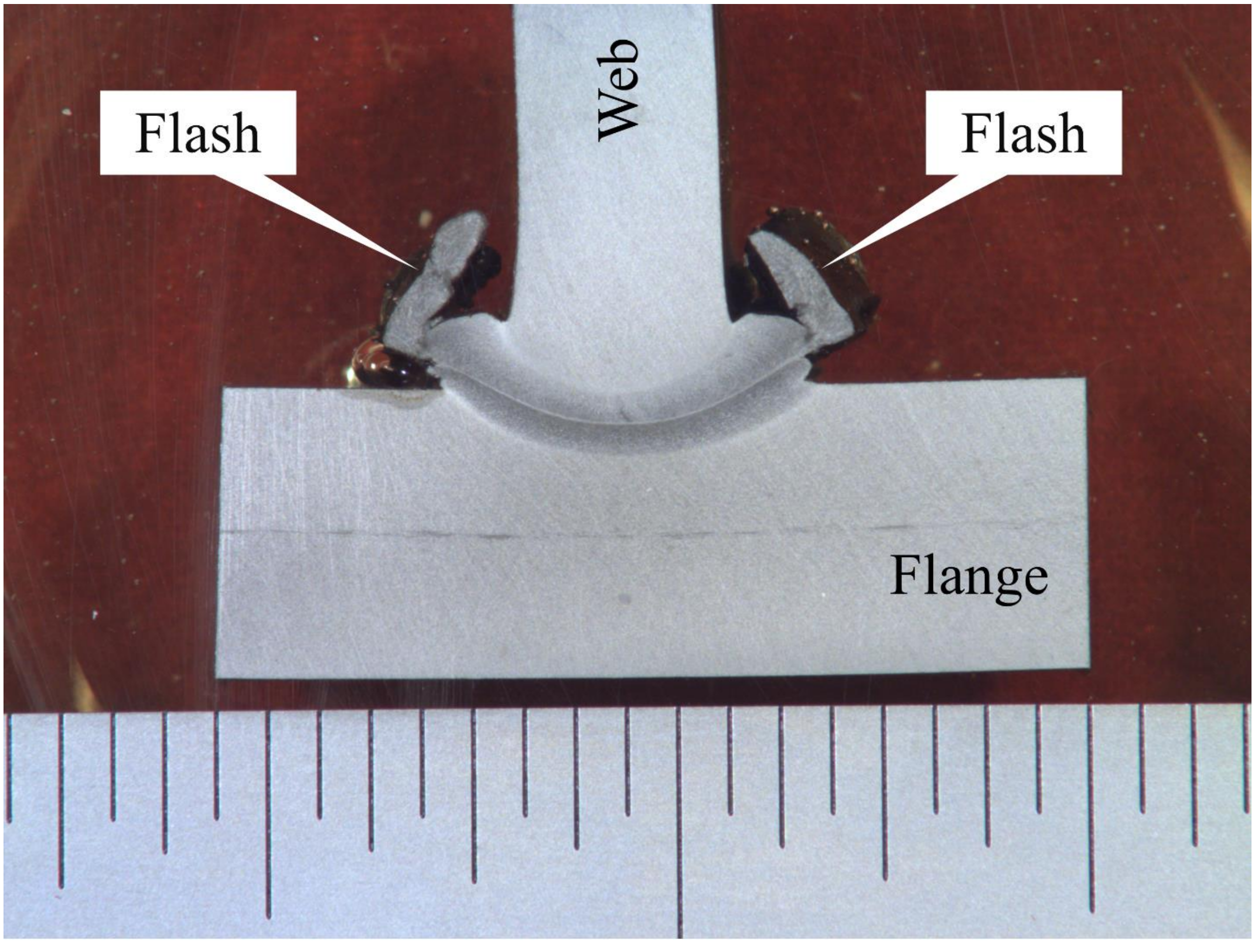

Source: FHWA.
Note: Scale is in increments of $^{1}/_{16}$ inch.

Figure 2. Photo. Macroetch of weld.

TENSION PROPERTIES

Tension testing was performed in accordance with ASTM Standard E8 to confirm the steel mechanical properties.(3) Four standard-sized, sheet-type tension specimens were taken from the tension flange of beam 1 after fatigue testing. The samples were taken from a flange near the support that experienced low stresses throughout the fatigue testing period. Strain was monitored with a clip-on extensometer over the 2-inch gauge length of the specimen. Due to software issues while running one of the tests, one specimen was discarded.

Figure 3 shows plots of the tension test results from the three valid specimens tested, and succinct results are presented in table 2. Based on testing averages, the beam specimen steel exhibited a 0.2-percent offset yield strength of 51.6 ksi and an ultimate strength of 71.8 ksi. The fracture location for specimen 2 was very close to one of the extensometer contact points; thus, the elongation percentage at failure for this specimen was not captured accurately by the extensometer readings. This is illustrated by the behavior shown for specimen 2 in the plot of figure 3. The average elongation percentage for the two specimens with valid fracture locations was 42.6 percent, and the average reduction in area was 71.8 percent.

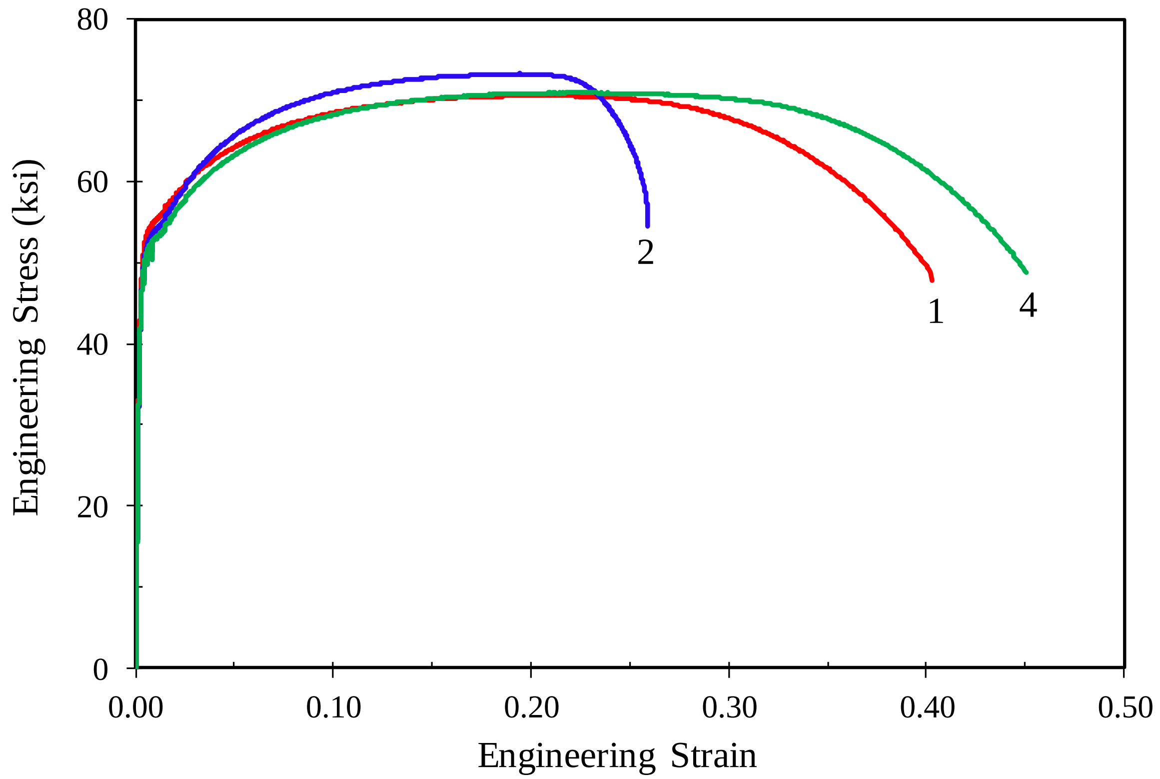

Source: FHWA.

Figure 3. Graph. Tension test results.

Table 2. Results of tensile tests.

Specimen	0.2 Percent Offset Yield (ksi)	Tensile Strength (ksi)	Extensometer Elongation (percent)	Reduction in Area (percent)
1	52.7	70.7	40.3	71.8
2	51.1	73.3	25.9	61.4
4	51.1	71.5	45.0	71.8

FATIGUE TESTING SETUP AND PROCEDURE

A 110-kip servo hydraulic actuator was used to load the simply supported beam specimens in four-point bending as illustrated in the load frame setup of figure 4. Beams were cyclically loaded with a sine wave function at rates between 1.5 and 1.75 Hz. A minimum load between 3.5 and 4 kip was used during cycling to prevent shifting and any unwarranted dynamic effects from occurring during testing. The maximum beam displacement was monitored throughout the test using a linear variable differential transducer within the actuator. Limits were set such that the actuator would turn itself off when the beam displacement increased 0.02 inch more than when the limit was turned on. Generally, it was possible to find budding cracks near the web–flange junction within the constant moment regions. Once cracks were discovered and marked, beams were cycled to failure. Typically, less than 5,000 additional cycles were enough at this point for a crack to extend well into the web of the beam specimen or for stability issues to occur due to asymmetrical loading caused by the ever-increasing loss of specimen cross section at the crack locations.

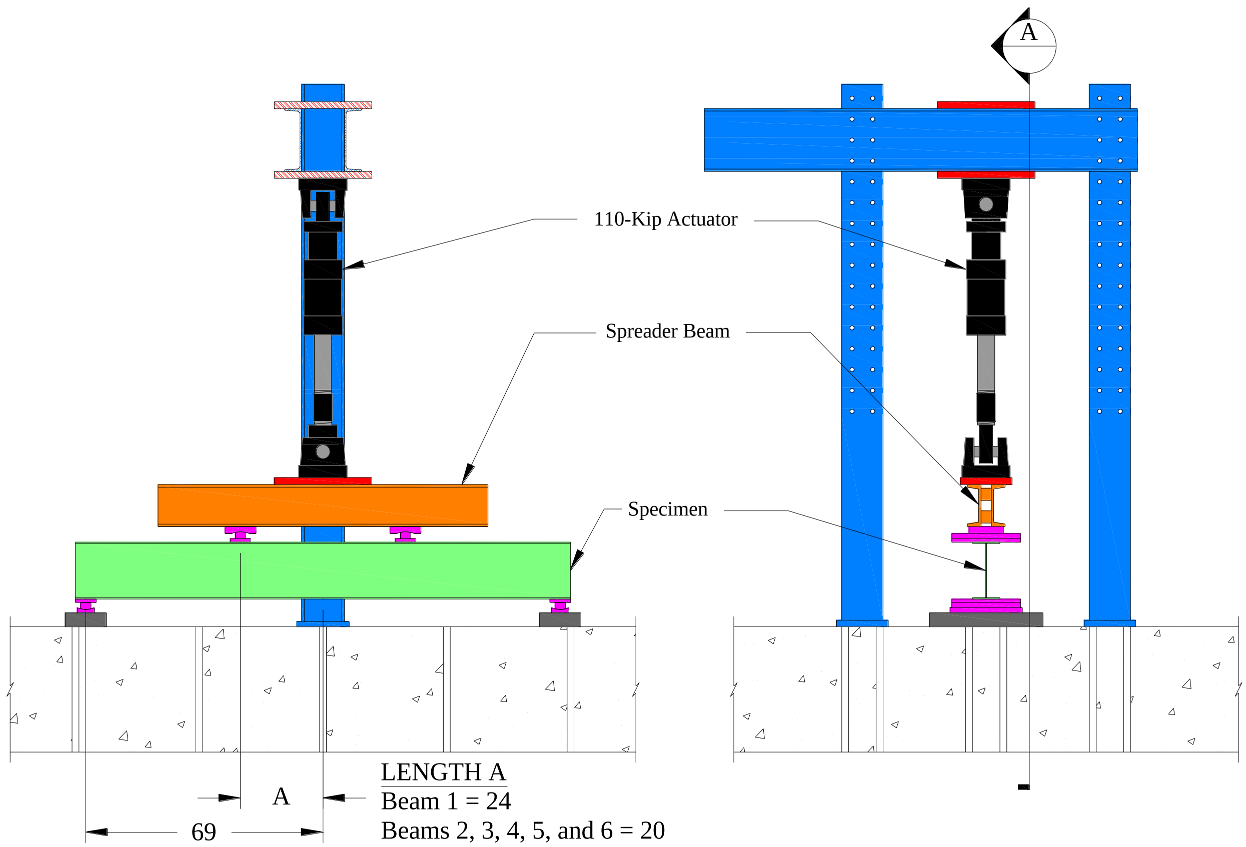

Source: FHWA.
Note: Units = inches.

Figure 4. Illustration. Fatigue testing load frame setup.

The first three beams tested were instrumented with strain gauges to ensure symmetrical loading. Strain gauges were placed on both sides of the web at three separate locations along the inside of the tension flange in the constant moment region and at midspan on the inside of the compression flange. Strains on average agreed with strains calculated using linear elastic beam theory.

The beam supports were 6 inches wide in the direction of the beam length, resulting in a span of 138 inches between support centers (figure 4). For the first beam test (i.e., beam 1), the span between the centers of the spreader beam load bearings was 48 inches. However, due to initial imperfections in the specimens, web slenderness, and an insufficient amount of torsional stiffness in the spreader beam, there sometimes were elastic stability issues that caused the actuator to move out-of-plane. To combat this, lateral braces at the beam supports were constructed using a steel bar and C-clamps as shown in figure 5. Wooden stiffeners were used at the supports to provide additional torsional and overturning stiffness at these locations as can also be seen in the same figure. A lateral torsional support was provided by bracing the beam compression flanges at midspan using a slender steel plate strip that was clamped to the compression flange on one end and to a load frame column on the opposite end as shown in figure 6. After testing of beam 1 was complete, the center-to-center distance between spreader beam load bearings was decreased to 40 inches to further remedy the stability issue encountered.

Source: FHWA.

Figure 5. Photo. Support lateral torsional bracing.

Source: FHWA.

Figure 6. Photo. Midspan lateral torsional bracing.

When conducting the first two beam tests (i.e., beams 1 and 2), the spreader beam bearings were detailed, as shown in figure 7, by clamping the specimen between two thick plates. Clamping the plates prevented the loading points from moving under the cyclic loading, and wooden stiffeners were used to prevent distortion to the beam from the clamping force. This setup proved adequate for testing beam 1. However, during testing of beam 2, an audible squeaking developed at one of the spreader beam load bearings on several occasions from slight movement between the specimen tension flange and the bottom clamping plate. The squeaking was eliminated by tightening the high-strength rods, thus increasing the clamping effect. This eventually led to a fretting failure of beam 2 as will be discussed later. Since fretting was undesirable, the load-bearing setup was simplified for beams 3 through 6. The revised setup eliminated the wood stiffeners, high-strength rods, and lower clamping plate and instead modified the upper plate so it could directly clamp to the specimen compression flange as seen in figure 6.

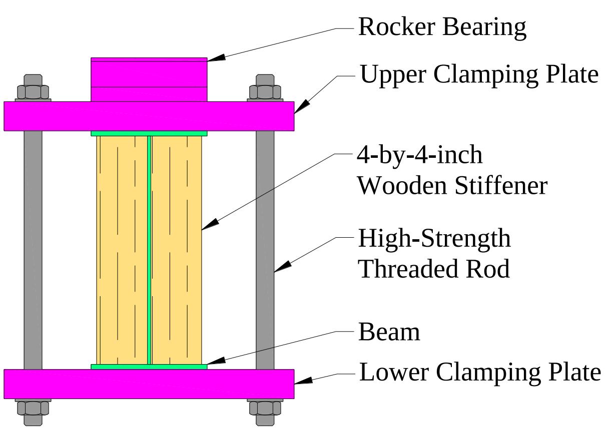

Source: FHWA.

Figure 7. Illustration. Bearing setup for beams 1 and 2.

FATIGUE TEST RESULTS

This section contains a brief discussion of the results for each individual beam test as well as a discussion and analysis of the results.

Table 3 gives the fatigue testing matrix for the beam specimens. The stress ranges given in the table correspond to the stress at the web–flange weld, or the stress at the inner surface of the tension flange, as calculated using elementary beam theory. Note that, prior to beginning testing, the fatigue resistance of the beams was unknown. It was assumed at the time that the fatigue resistance would fall somewhere between an AASHTO category A detail and a category B fatigue detail, inclusive.(1) The choice of test stress ranges for the later tests was thus partially guided by the results from earlier tests. The desire was to achieve a fatigue failure for each beam test at less than 2 million cycles due to time considerations. A high stress range was thus used in the first test to avoid a runout situation that might have occurred because of loading below the constant amplitude fatigue limit for a category A detail.

Table 3. Beam specimen fatigue test matrix.

Beam ID	Actuator Minimum Load (kip)	Actuator Maximum Load (kip)	Load Ratio	Stress Range (ksi)	Cycles to Failure	Failure Mode
1	3.0	78.0	0.04	29.4	705,098	Flange tip
2	4.0	53.6	0.07	21.1	885,955	Fretting
3	3.6	54.1	0.07	21.5	2,167,158	Weld
4	3.6	54.1	0.07	21.5	1,484,999	Weld
5	3.5	59.1	0.06	24.7	856,622	Flange tip
6	3.5	59.1	0.06	24.7	1,061,520	Weld

BEAM 1

The displacement limit for beam 1 tripped at around 702,000 load cycles. Once restarted, a large crack was noted approximately 3 inches inside the load-bearing clamping plate edge. Cycling was discontinued at 705,098 cycles when the actuator pushed sideways inside the load frame due to the now asymmetrical cross section. Figure 8 shows a picture of the entire fracture surface. As can be seen from the overall perspective, the right side of the flange had completely fractured, though the left side of the flange and web were only partially fractured. Also shown on the overall perspective is a dashed arc that indicates nearly equal crack growth across the left half of the flange and up the web, indicating that this crack likely initiated at the right flange tip. The fracture surface at the right flange tip had impact damage from the fatigue cycling, and a zoomed-in view notes the likely crack origin was a small flaw from the shear-cut edge.

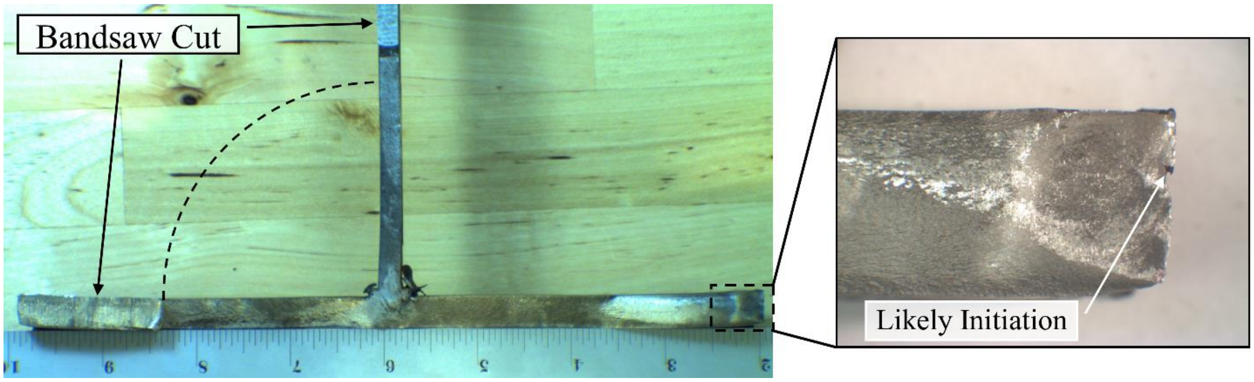

Source: FHWA.

Figure 8. Photo. Beam 1 fracture surface.

BEAM 2

The displacement limit for beam 2 tripped at 885,073 load cycles. Once restarted, a crack was observed in the tension flange near the inside edge of the load-bearing clamping plate. Instability of the actuator occurred shortly thereafter at 885,955 cycles, at which point the cycling was stopped. The observed crack plane was directly parallel to the edge of the clamping plate. As mentioned previously, the clamp-type load bearing for beam 2 oftentimes had to be tightened to halt a squeaking noise that developed as loading commenced. Failure was determined to be caused by fretting of the clamping plate. Figure 9 shows a photo of the web-to-tension flange junction where the crack was observed. The photo indicates that the ratchet marks on the bottom of the flange were likely five to six small fretting cracks that coalesced together, and the fatigue crack grew upward toward the web-to-tension flange junction.

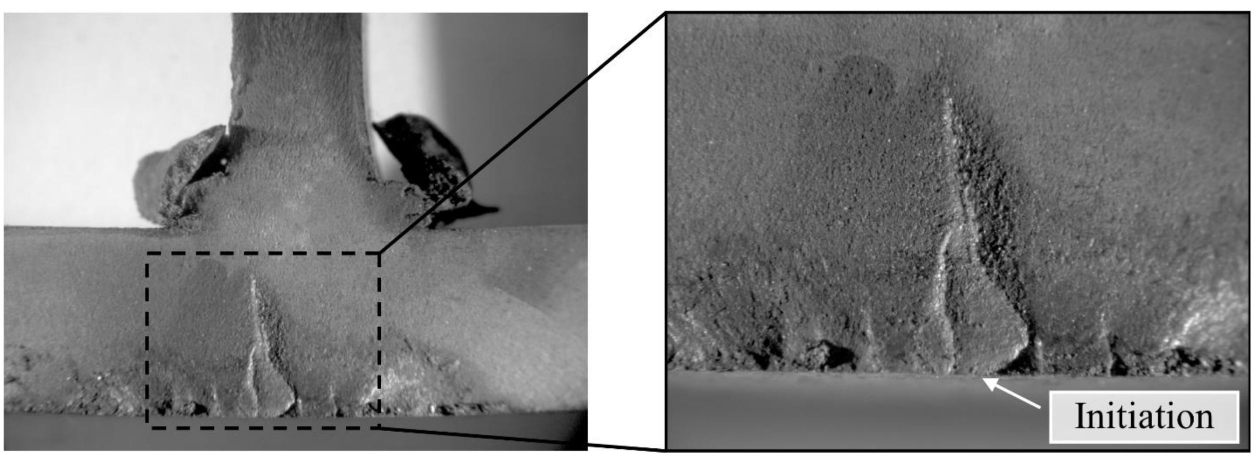

Source: FHWA.

Figure 9. Photo. Beam 2 web–flange junction fracture surface.

BEAM 3

The displacement limit for beam 3 tripped at 2,157,969 load cycles. Once restarted, cracks were observed at multiple locations. The largest of the cracks occurred in the web–flange junction approximately 10 inches inside of the inside edge of the left load-bearing plate. Failure progressed most rapidly at this location. An additional smaller web–flange crack was observed almost directly under the left support. A third crack was observed on the edge of the flange approximately 2 inches from the right load-bearing plate within the constant moment region of the beam. Actuator instability occurred at 2,167,158 load cycles, and the test was terminated. Figure 10 shows a zoomed-in view of the web-to-tension flange junction of the largest crack. Semicircular fatigue crack growth rings obviously emanate from the weld flash on the right-hand side of the weld, indicating the flash was the initiation point.

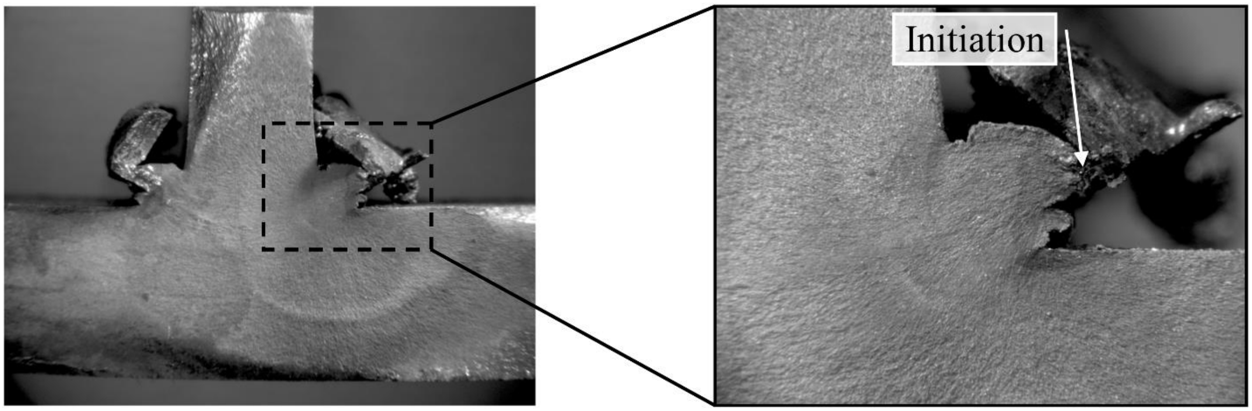

Source: FHWA.

Figure 10. Photo. Beam 3 web–flange junction fracture surface.

BEAM 4

The displacement limit for beam 4 tripped at 1,483,802 load cycles. Once restarted, complete fracture of one-half of the flange was observed approximately 18 inches inside of the centerline of the left load bearing. The test was stopped due to pending instability of the actuator at 1,484,999 load cycles. Figure 11 shows a zoomed-in view of the web-to-tension flange junction. The overall crack was a coalescence of three smaller cracks at slightly different locations along the beam length. Two of the small cracks initiated at each tension flange tip and grew inward to the weld, and the third crack initiated at the web-to-tension flange weld. The view in the picture focuses on the weld, and the other cracked planes appear out of focus because they are not coincident. Fatigue growth rings indicate the crack in the weld initiated from the weld flash.

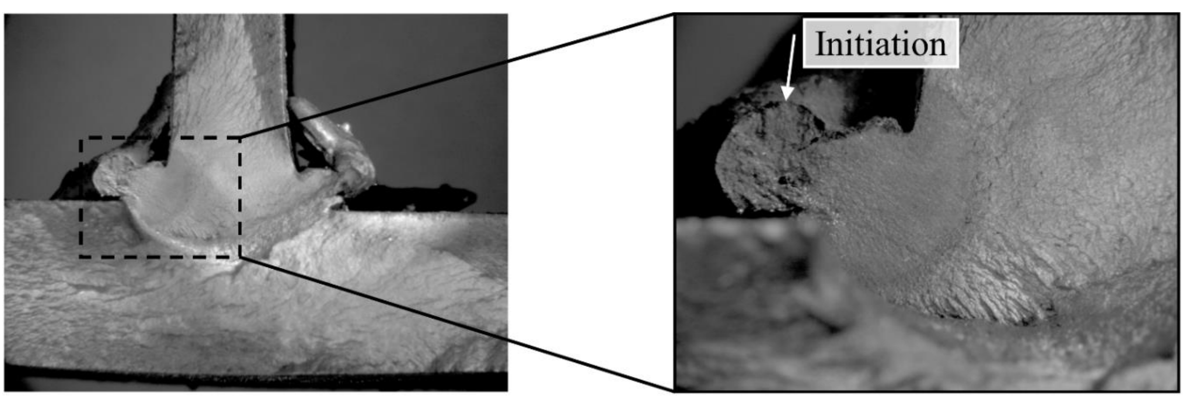

Source: FHWA.

Figure 11. Photo. Beam 4 web–flange junction fracture surface.

BEAM 5

The actuator turned itself off at 856,622 load cycles when testing beam 5. At this time, a full flange fracture was observed that extended approximately one-third of the way up the web. A view of the full fracture surface is shown in figure 12. Large fatigue growth striations can be seen near the left flange tip and near the crack tip in the web. A dashed arc is drawn between these last striations, indicating a growth origin near the weld. However, complete fracture of the right side of the flange indicates the crack originated from the right flange tip, grew toward the weld, and then continued to grow into the left side of the flange and up the web. A zoomed-in view of the flange tip is provided, indicating that the initiation of the crack was a discontinuity from shear cutting at the lower left corner of the flange tip. Finally, the left flange tip was necked through the plate thickness, indicating this was a ductile overload fracture, and was the last event that had tripped the limit.

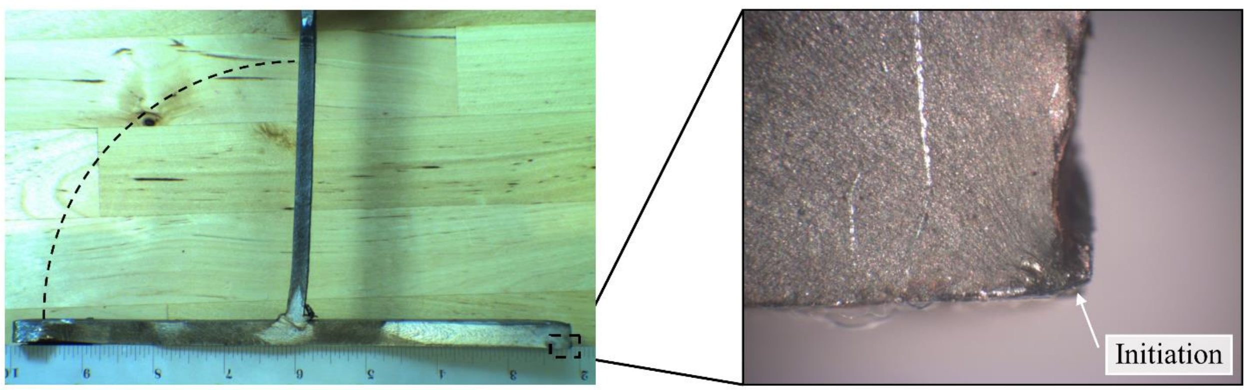

Source: FHWA.

Figure 12. Photo. Beam 5 fracture surface.

BEAM 6

The displacement limit for beam 6 was tripped at 1,057,914 load cycles. A crack was detected, this time at the web–flange junction approximately 15 inches on the inside edge of the load-bearing plate. Restarting the test to further propagate the crack resulted in actuator instability at 1,061,520 load cycles. The test was stopped at this point. Figure 13 shows the web-to-tension flange junction where the crack was first observed. Fatigue crack growth indicates initiation started in the weld flash on the right side.

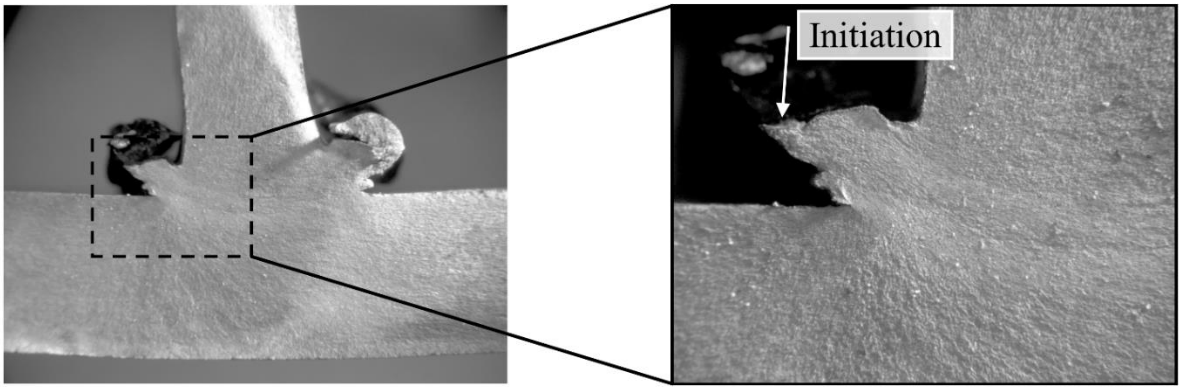

Source: FHWA.

Figure 13. Photo. Beam 6 web–flange junction fracture surface.

DISCUSSION AND ANALYSIS

The fatigue data are plotted in stress versus cycles to failure format consistent with the AASHTO fatigue design philosophy in figure 14. The three weld failures are plotted as blue triangles falling between category A and B performance. However, to be consistent with the AASHTO methodology, a lower-bound resistance is shown as the heavy, blue dashed line in the figure representing the lower 95-percent confidence limit. The lower-bound resistance is less than category B. For completeness, the one fretting failure and two flange tip failures are also plotted on the graph.

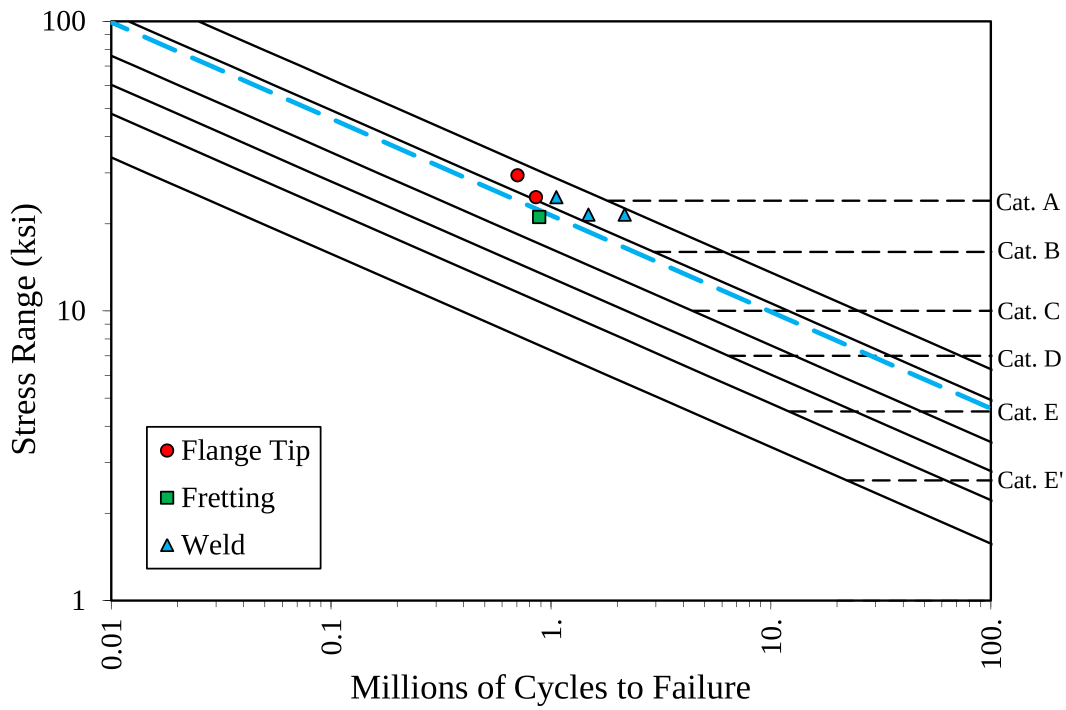

Source: FHWA.
Cat. = category.

Figure 14. Graph. Beam test results with AASHTO fatigue life curves.

CONCLUSIONS

This research was performed to develop preliminary fatigue design recommendations for the use of HF-welded steel I-beams in bridge design. The HF welds were used in joining the web and flanges of the I-beam. Historical fatigue data have found longitudinally loaded web-to-flange welds are category B details, whether joined by fillet or CJP welds.[(4)] The lower bound of the three HF welds was less than category B, indicating HF welds have lesser fatigue strength than conventional welds. However, a statistically significant pool of HF weld failures is needed to more confidently make this conclusion.

Future work should consider removal of the flash from the web–flange junction after completion of the HF welding fabrication process. The three HF weld failures originated from the flash, and removing it could eliminate flaws and possibly increase the fatigue resistance. Furthermore, strict adherence to fabrication tolerances may provide benefits. Fabrication tolerances for the specimens tested in this research were questionable in some instances with regard to the perpendicularity of the web–flange junction. In some instances, this led to lateral instability issues during testing. Lastly, the beam sections tested were quite small, with a total depth of approximately 16 inches and flange thickness of 0.35 inch. Typical bridge designs use much larger sections, and additional testing should also be performed to ensure there are not scale effects.

REFERENCES

1. AASHTO. (2014). *AASHTO LRFD Bridge Design Specifications*. 7th ed. American Association of State Highway and Transportation Officials, Washington, DC.

2. ASTM Standard A769/A769M. (2010). "Standard Specification for Carbon and High-Strength Electric Resistance Forge-Welded Steel Structural Shapes." *Book of Standards Volume 01.04*. ASTM International, West Conshohocken, PA.

3. ASTM E 8/E 8M-08. (2008). "Standard Test Methods for Tension Testing of Metallic Materials." *Book of Standards Volume 03.01*. ASTM International, West Conshohocken, PA.

4. Keating, P.B. and Fisher, J.W. (1986). *Evaluation of Fatigue Tests and Design Criteria on Welded Details*, Report No. 286, National Cooperative Highway Research Program, Transportation Research Board, Washington, DC.

HRDI-40/02-18(WEB)E